Effects of polarization on intersubband transitions of $Al_xGa_{1-x}N$/GaN multi-quantum wells*

Tian Wu(田 武)[a], Yan Wei-Yi(鄢伟一)[a], Xiong Hui(熊 晖)[a]†, Dai Jian-Nan(戴江南)[a], Fang Yan-Yan(方妍妍)[a], Wu Zhi-Hao(吴志浩)[a], Yu Chen-Hui(余晨辉)[b], and Chen Chang-Qin(陈长清)[a]

[a] *Wuhan National Laboratory for Optoelectronics, College of Optoelectronic Science and Engineering, Huazhong University of Science and Technology, Wuhan* 430074, *China*

[b] *Jiangsu Key Laboratory of ASIC Design, Nantong University, Nantong* 226019, *China*

(Received 3 September 2012; revised manuscript received 21 October 2012)

The effects of polarization and related structural parameters on the intersubband transitions of AlGaN/GaN multi-quantum wells (MQWs) have been investigated by solving the Schrödinger and the Poisson equations self-consistently. The results show that the intersubband absorption coefficient increases with increasing polarization while the transition wavelength decreases, which is not identical to the case of the interband transitions. Moreover, it suggests that the well width has a greater effect on the intersubband transitions than the barrier thickness, and the intersubband transition wavelength of the structure when doped in the barrier is shorter than that when doped in the well. It is found that the influences of the structural parameters differ for different electron subbands. The mechanisms responsible for these effects have been investigated in detail.

Keywords: intersubband transition, polarization, electron subband levels, AlGaN/GaN quantum well

PACS: 73.21.Fg, 73.22.–f, 71.55.Fq **DOI:** 10.1088/1674-1056/22/5/057302

1. Introduction

In recent years, the III–nitride materials have received much attention because of their potential usefulness in ultraviolet and blue lighting, detection,[1] high density optical storage systems, full-color displays, chemical sensors, and medical applications.[2,3] While most of the contemplated applications are in the visible and ultraviolet spectral region and based on their interband transitions, interest has been increasing in infrared applications based on their intersubband transitions (ISBT).[4–7] Compared to GaAs/AlGaAs and InGaAs/AlInAs, AlGaN/GaN multi-quantum wells (MQWs) have many advantages. First, the large conduction band offset ($\sim$ 1.7 eV) allows the design of optoelectronic devices based on the intersubband transitions working in the wavelength region of 0.7–14 μm,[8] which sufficiently covers the exploitation of near-infrared intersubband transitions, especially in the communication region. Second, the strong electron–phonon interaction in these materials due to their highly polar nature yields particularly short intersubband relaxation time ($\sim$ 140 fs), which shows the prospect of ultrafast intersubband devices operating at multi-Tbit/s data rates.[9] Moreover, it is the only material that can be used to integrate infrared detectors with ultraviolet photodetectors on the same wafer, which is meaningful in military applications. These properties make AlGaN/GaN MQWs one of the most promising materials for infrared devices, such as ultrafast fiber-optic modulators and detectors operated in the atmospheric communication.[10,11]

However, the strong spontaneous polarization and piezoelectric polarization of AlGaN materials have big impacts on the energy bands and the performance of the optoelectronic devices, which adds more difficulties to the design of the intersubband devices. Although many efforts have been made to study the influences of Al mole composition, barrier thickness, and well width on the intersubband transition wavelength,[12,13] few papers have reported the effects of such structural parameters as barrier thickness, well width, Al mole composition, and doping on the properties of intersubband transitions, electron distributions, and electron subband levels in the AlGaN/GaN MQWs systematically. In this paper, the influences of polarization and related parameters on the properties of AlGaN/GaN MQWs are investigated numerically by solving the Schrödinger and the Poisson equations self-consistently. The simulated results reveal the effects of polarization on the electron distribution and the electron subband levels, which are quite important to the designers of devices based on the intersubband transitions.

2. Theoretical calculation

The absorption coefficient of the intersubband transitions in the conduction band of AlGaN/GaN MQWs can be ex-

*Project supported by the National Basic Research Program of China (Grant Nos. 2012CB619302 and 2010CB923204), the National Natural Science Foundation of China (Grant Nos. 60976042, 51002058, and 11104150), and the China Postdoctoral Science Foundation (Grant No. 20100480064).

†Corresponding author. E-mail: hsiung.hust@gmail.com

© 2013 Chinese Physical Society and IOP Publishing Ltd

pressed as a function of w in the following form:[14]

$$a(w) = \frac{w}{L}\sqrt{\frac{\mu_0}{\varepsilon_0\varepsilon_r}}\sum_{m>n}\frac{|M_{mn}|^2(N_n - N_m)(\hbar/\tau)}{(E_m - E_n - \hbar w)^2 + (\hbar/\tau)^2}, \quad (1)$$

where μ_0 is the permeability in a vacuum, ε_0 is the dielectric constant in a vacuum, ε_r is the relative dielectric constant, L is the width of one period of the quantum well, $\hbar$ is the reduced Planck constant, τ is the dephasing time in the well material and is assumed to be 20 fs in the programs.[15] M_{mn} is the dipole matrix, which is given by

$$M_{mn} = \int_{-L/2}^{L/2}\varphi_m^*(z)ez\varphi_n(z)\,\mathrm{d}z, \quad (2)$$

where e is the electronic charge. The N_i is the total number of electrons residing on the i-th subband level, and E_i and φ_i ($i = m,n$) are the energy level and the wave function of the i-th subband, respectively. They are obtained by solving the Schrödinger and the Poisson equations self-consistently[16]

$$-\frac{h^2}{2}\frac{\mathrm{d}}{\mathrm{d}z}\left[\frac{1}{m^*(z)}\frac{\mathrm{d}}{\mathrm{d}z}\varphi_i(z)\right] + [V(z) + \Delta E(z) + V_{xc}(z) - e\phi_H(z)]\varphi_i(z) = E_i\varphi_i(z), \quad (3)$$

$$V_{xc}(z) = -0.985\frac{e^2}{4\pi\varepsilon_0\varepsilon_r}n^{1/3}(z) \times\left\{1 + \frac{0.034}{a_H^* n^{1/3}(z)}\ln[1 + 18.376a_H^* n^{1/3}(z)]\right\}, \quad (4)$$

$$\frac{\mathrm{d}}{\mathrm{d}z}\left[\varepsilon_0\varepsilon_r\frac{\mathrm{d}}{\mathrm{d}z}\phi_H(z)\right] = -e[N_D^+(z) - n_{2D}(z) - n_{3D}(z)], \quad (5)$$

where z is the space coordinate parallel to the growth direction, and $m^*(z)$ is the position-dependent effective mass. Here $V(z)$ is the potential caused by the polarization field and can be calculated by

$$V(z) = ezF(z), \quad (6)$$

where $F(z)$ is the electrostatic field caused by the polarization, which can be obtained by the equations in Ref. [17]; $\Delta E(z)$ is the conduction band offset; $\phi_H(z)$ is the Hartree potential due to the electrostatic interaction; $V_{xc}(z)$ is the exchange–correlation potential; $a_H^* = 4\pi\varepsilon_0\varepsilon_r\hbar^2/m^*(z)e^2$; $N_D^+(z)$ is the ionized donor density; and $n_{2D}(z)$ is the two-dimensional (2D) electron density in all subbands.

Under the equilibrium condition, n_{2D}, n_{3D}, and N_i are given by[15]

$$n_{2D}(z) = \sum_i n_{2D_i}(z) = \sum_i \frac{m^* kT}{\pi\hbar^2}|\varphi_i(z)|^2 \times \ln\left[1 + \exp\left(\frac{E_F - E_i}{kT}\right)\right], \quad (7)$$

$$n_{3D}(z) = N_c(z)F_{1/2}\left(\frac{E_F - E_i}{kT}\right), \quad (8)$$

$$N_i = \int n_{2D_i}|\varphi(z)|^2\,\mathrm{d}z, \quad (9)$$

where k is the Boltzmann constant, T is the absolute temperature, E_F is the Fermi level, $N_c(z)$ is the three-dimensional (3D) density of states, $F_{1/2}$ is the Fermi–Dirac integral, and n_{2D_i} is the 2D density of the i-th state. In the calculation, the initial potential profile is assumed to be $V(z) + \Delta E(z)$ and the center of the barrier is used as the potential reference point.

3. Results and discussion

In the calculation, the band gaps of GaN and AlN are chosen to be 3.42 eV and 6.12 eV, respectively, and the band-offset ratio is assumed to be 0.65/0.35.[18] Based on the assumption of the periodic potential model, the charge neutrality condition is adopted, and the potential drop across one period induced by the polarization is assumed to be zero.[19] The basic structure used in the program is 5 nm $Al_{0.35}Ga_{0.65}N$/3 nm GaN MQWs deposited on a GaN template, which is identical to the structure reported in Ref. [6]. The doping density of SiH_4 in the GaN well is equal to 1×10^{19} cm^{-3}. Due to ignoring the coupling between the quantum wells, the profiles of the quantum wells are the same. So in the program, one quantum well is calculated, which does not affect the properties of the intersubband transitions. The calculation results are shown in Fig. 1, which reveals the conduction band and the electron subband wave functions in Fig. 1(a) and the absorption coefficient in Fig. 1(b). The wavelength of the intersubband transition from the first electron subband level (e_1) to the second subband level (e_2) is 4.12 μm, which is similar to the experimental result of 4.1 μm.[6] So this program can be used to investigate the intersubband transitions in AlGaN/GaN MQWs. The work shown below is based on this structure.

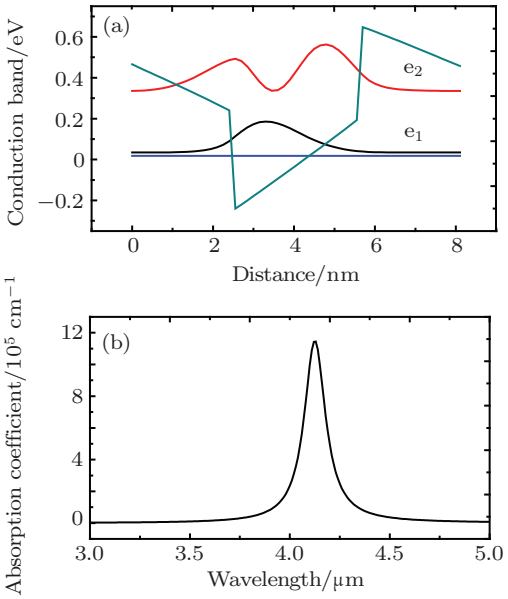


Fig. 1. (color online) (a) Conduction band of $Al_{0.35}Ga_{0.65}N$/GaN MQWs and moduli square of the first two wave functions under zero applied electric field. (b) Absorption coefficient of e_1–e_2 ISBT in the $Al_{0.35}Ga_{0.65}N$/GaN MQWs.

3.1. Effects of spontaneous and piezoelectric polarizations on the intersubband transitions

Four cases with different polarizations are studied in this paper: case 1 with no polarization in the whole system, case 2 considering only the spontaneous polarization, case 3 thinking about only the piezoelectric polarization, case 4 taking spontaneous and piezoelectric polarizations into account simultaneously. The electrostatic fields and the positions of the subband levels of these cases are shown in Table 1.

Table 1. Calculated results of subband levels, electrostatic field, and dipole matrix.

	Case 1	Case 2	Case 3	Case 4
e_1/eV	0.0871	0.0402	0.0588	–0.0292
e_2/eV	0.3568	0.3373	0.3426	0.3163
Field in the well/MV·cm^{-1}	0	–1.36	–1	–2.4
$\lvert M_{mn}\rvert/10^{28}$	1.37	1.23	1.29	1.08

As shown clearly in Fig. 2, the absorption coefficient and the wavelength are significantly sensitive to the polarizations. Compared to case 1, the other cases all have larger absorption coefficients and shorter wavelengths. Furthermore, the absorption coefficient for case 4 is almost 8 times larger than that for case 1, and the transition wavelength of case 4 is shorter than that of the other cases. These two phenomena are opposite to the interband transitions in the AlGaN-based LED, in which the absorption coefficient is decreased and the transition wavelength is red shifted as the polarization field is increased.[20] In order to probe the origins of this contradictory phenomenon, the conduction bands, electron subband levels, electron densities, electrostatic fields in the well, and the dipole matrix are investigated in detail.

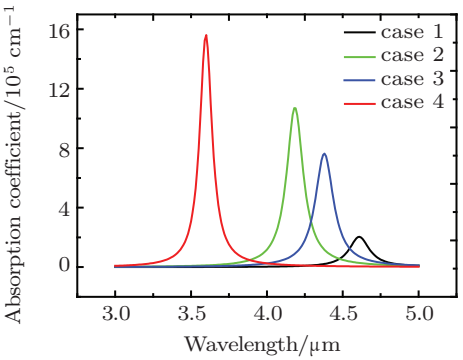


Fig. 2. (color online) Absorption coefficients of e_1–e_2 ISBT in $Al_{0.35}Ga_{0.65}N$/GaN MQWs for the four cases.

As shown in Fig. 3(a), the polarization field leads to a tilt of the band, and the slope of the tilt is proportional to the field, which means that the height of the triangular well becomes higher and the confinement of electrons becomes stronger when the polarization field is increased. To explain this, the relationship between the electron subband levels and the electrostatic field is shown in Fig. 3(b). The positions of e_1 and e_2 are lowered with the increasing electrostatic field in the quantum well in all four cases, which means that the confinement is enhanced and the effective barrier height becomes higher. Moreover, the decline of e_1 is steeper than that of e_2, which means that the effect of polarization on e_1 is greater than that on e_2. As a result, the energy space between e_1 and e_2 is increased with the enhancement of the electrostatic field. These results are in line with Fig. 2, which demonstrates that the transition wavelength is blue shifted with the increase of the polarization.

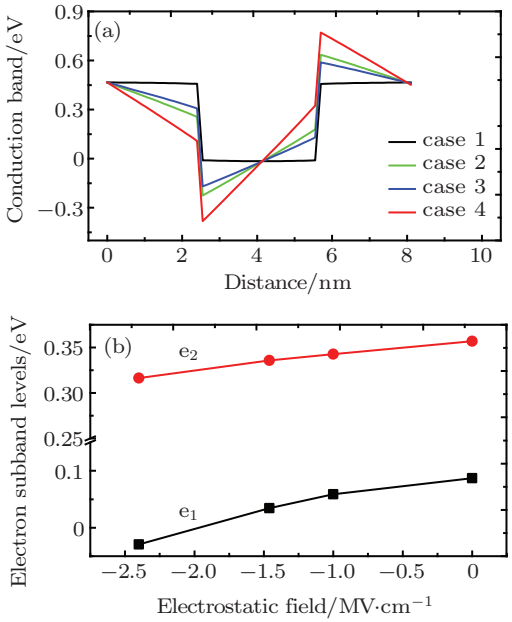


Fig. 3. (color online) (a) Schematic diagram of conduction bands and (b) electron subband levels as a function of electrostatic field for the four cases.

In addition, figure 2 shows that the absorption coefficient is increased when the polarization field is enhanced in the GaN quantum well. However, as shown in Table 1, the dipole matrix M_{mn}, which represents the overlap of the wave functions of e_1 and e_2, is decreased when the polarization field is increased. This means that the relative position of the centers of these two wave functions is enlarged when the field is increased, which leads to the decrease of the absorption coefficient. This is not identical to the simulated results shown in Fig. 2. In order to explain this phenomenon, the electron distribution in the well is investigated.

Figure 4 shows the electron distributions in the quantum well for the four cases, which indicates that the electron density increases with increasing polarization. This may be attributed to two reasons. Firstly, the tilt of the band gives rise to the triangular well, which increases the effective barrier height, resulting in more electrons confined in the well. Secondly, the band bending raises the Fermi level, resulting in a decrease of the active energy of the dopant. Therefore, more electrons are located in the well, which corresponds to

a method that has been proposed to improve the doping efficiency by using the polarization in the superlattice.[21] Although the dipole matrix M_{mn} can be slightly reduced when the polarization field is increased, the electron density in the well is increased, and this increase is more dramatic. As a result, the absorption coefficient is increased when the polarization field is enhanced.

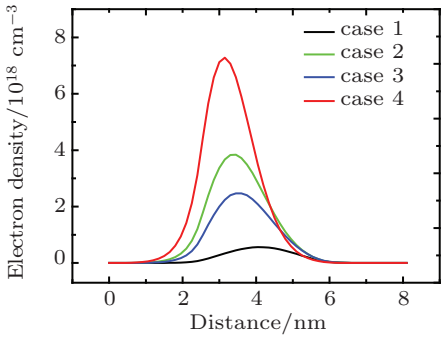


Fig. 4. (color online) Electron density of $Al_{0.35}Ga_{0.65}N$/GaN MQWs with different polarization.

Given the phenomena discussed above, we know that the polarization significantly influences the intersubband transitions in the MQWs, which leads to a blue shift of the transition wavelength and enhances the subband transition. Therefore, parameters such as barrier thickness, well width, Al mole composition of the barrier, and doping, which are related to the polarization, also affect the properties of the intersubband transitions. The effects of these parameters on the intersubband transitions, electron distributions, and electron subband levels will be discussed in detail.

3.2. Effects of barrier thickness and well width on the intersubband transitions

As reported in Ref. [16], the polarization field is a function of both the barrier thickness and the well width, which suggests that the barrier thickness and the well width could also affect the polarization field in MQWs. In order to shed light on the effects of these two parameters on the intersubband transitions, the structure is investigated with the barrier thickness varied from 3 nm to 9 nm and the well width changed from 2 nm to 6 nm. Table 2 shows the calculated results of the structures with the barrier thickness varied from 3 nm to 9 nm while the well width is fixed at 3 nm.

Table 2. Simulated results of the structure with varied barrier thickness.

Thickness/nm	3	4	5	6	7	8	9
Wavelength/μm	3.5190	3.5589	3.5982	3.6377	3.6978	3.7753	3.8535
Field/MV·cm^{-1}	–1.5200	–2.1700	–2.3700	–2.5300	–2.6500	–2.7500	–2.8400
e_1/eV	0.0181	0.0037	–0.0292	–0.0362	–0.1646	–0.0633	–0.0667
e_2/eV	0.3964	0.3530	0.3163	0.3055	0.2938	0.2660	0.2559
e_3/eV	–[a)]	–	0.5564	0.5112	0.4745	0.4259	0.4047
e_4/eV	–	–	–	–	–	0.6352	0.5916

[a)] The "–" stands for no existence of this electron subband level.

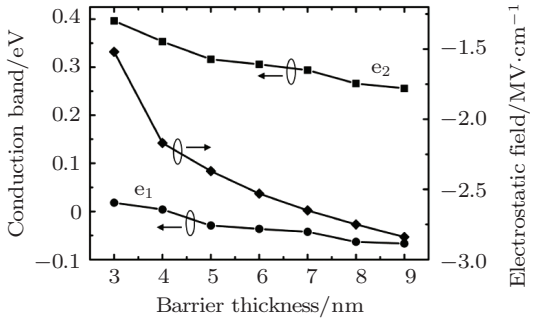


Fig. 5. Electron subband levels and electrostatic field of AlGaN/GaN MQWs with different barrier thickness.

As shown in Table 2, it is evident that as the barrier thickness is enlarged, the number of confined subband levels is increased, which can be attributed to the enhanced electrostatic field in the well when the barrier thickness is increased, as shown in Fig. 5. The electrostatic field enhances the tilt of the conduction band and adds to the confinement of subband levels. Although the number of subband levels is increased, the barrier height changes only slightly. As a result, the energy space between e_1 and e_2 is decreased. Therefore, the wavelength is red shifted.

The intersubband transitions occur in the quantum well. Therefore, the well width is an important parameter. As shown in Fig. 6(a), the transition wavelength red shifts as the well width increases from 2 nm to 6 nm, which may result from the reduced confinement of electrons when the width is enlarged. As shown in Fig. 6(b), the relative positions of electron subband levels become closer with increasing well width, which indicates that the confinement is decreased. However, the absorption coefficient increases with increasing well width. According to Eq. (1), the absorption coefficient mainly depends on the dipole matrix M_{mn} and the densities of electrons residing in e_1 and e_2. However, the calculated results show that M_{mn} only changes slightly from -9.91×10^{-29} to -1.16×10^{-28} when the well width is increased from 2 nm to 6 nm. Therefore, the absorption coefficient is determined predominantly by the electron densities of e_1 and e_2. The density distribution of electrons located on the basic level is shown in Fig. 6(c),

which reveals that the density of electrons is increased with increasing well width. Therefore, the absorption coefficient is increased. This may result from the fact that the number of dopant atoms is increased when the well width is increased, which can induce more electrons into the well. Moreover, due to the influence of fixed charge located at the interface, electrons are unevenly distributed in the well and more electrons reside in the triangular well, resulting in more electrons located on e_1. As a result, the absorption coefficient increases with increasing well width.

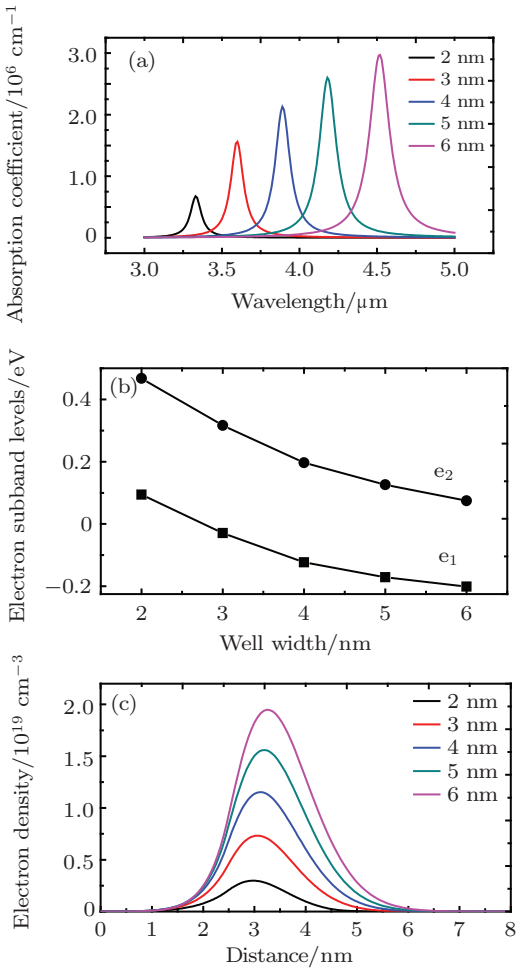


Fig. 6. (color online) (a) Absorption coefficients, (b) electron subband levels, and (c) electron densities of the structures with well widths of 2 nm, 3 nm, 4 nm, 5 nm, 6 nm.

As discussed above, it is clear that the intersubband transition wavelength is red shifted with the increases of the barrier thickness and the well width, and the well width influences the wavelength more distinctly than the barrier thickness, which is similar to the result in Ref. [22]. So it is very important to make sure that the well widths vary minimally when preparing intersubband devices based on the AlGaN/GaN MQWs. This also suggests that ensuring uniformity of the well widths is an effective way to reduce the full width at half maximum of the intersubband absorption spectrum.

3.3. Effect of Al mole composition of barrier on the intersubband transitions

The Al mole composition of the barrier is another important parameter that affects the transition wavelength. On one hand, the Al mole composition influences the barrier height, which is directly related to the confinement of electrons in the well. On the other hand, the Al mole composition determines the crystal lattice, which affects the polarization of the barrier. So the transition properties can be tuned by changing the Al mole composition of the barrier. The effects of the Al mole composition are studied by varying it from 0.15 to 0.75. As shown in Fig. 7(a), the wavelength is blue shifted and the absorption coefficient becomes bigger when the composition is increased from 0.15 to 0.75. From Fig. 7(b), it is clear that the position of e_1 is lowered while that of e_2 is lifted, resulting in the blue shifts of the transition wavelength. The opposite behaviors of e_1 and e_2 can be explained by probing the effects of the Al mole composition on the potential profile of a quantum well. Because e_1 is confined in the triangular well, it is affected most by the polarization. So with the Al mole composition increased, which could increase the polarization field of the well, the position of e_1 is lowered. On the other hand, e_2 is located in the rectangular well and affected predominantly by the barrier height. When the barrier height is increased, the position of e_2 goes up. Therefore, the Al mole composition of the barrier has different influences on e_1 and e_2, which results in a significant change of the transition wavelength.

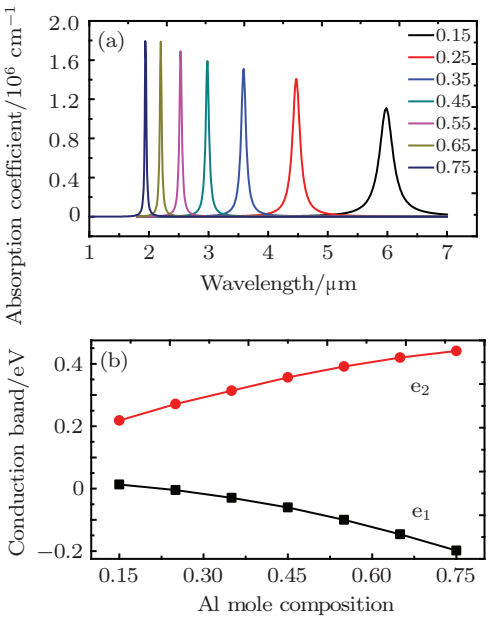


Fig. 7. (color online) (a) Absorption coefficients of the structures with different Al compositions; (b) electron subband levels in the MQWs with different Al compositions in the barrier.

3.4. Effect of doping on the intersubband transitions

Based on Fermi's golden rule, the intersubband transitions depend on the electron subband levels, especially the

electron density distribution in the well.[23] From the discussion above, the electron density in the well affects the absorption coefficient significantly. So the doping density of Si is also an important parameter of the intersubband devices. Although many papers have reported on the effects of doping density on the intersubband transitions in MQWs,[24,25] few have comprehensively investigated the effects of doping position and doping density on the transitions. In this part, the effects of doping position and doping density on the intersubband transitions in the basic structure will be studied in detail.

As shown in Fig. 8(a), the absorption coefficient of e_1–e_2 for doping in the barrier is almost double of that for doping in the well, while the wavelength of doping in the barrier is shorter than that of doping in the well. This can be attributed to two reasons. First, more electrons are located in the well when the dopant is in the barrier, as shown in Fig. 8(b). Due to the barrier and the well having the same Fermi level, donors in the barrier can be ionized into the conduction band of GaN, suggesting a higher ionization efficiency for doping in the barrier than that for doping in the well.[26] Since more electrons are in the well when the dopant is in the barrier, the wavelength blue shifts due to many body effects, which will be interpreted below. These results are in good agreement with the experimental results reported in Ref. [27], in which the results suggest that the wavelength is shorter when doping in the barrier and the absorption is also larger. However, the change is small, which may be attributed to the poor crystal quality when doping the barrier. So a lot of papers have reported the advantages of doping the well.[28–30]

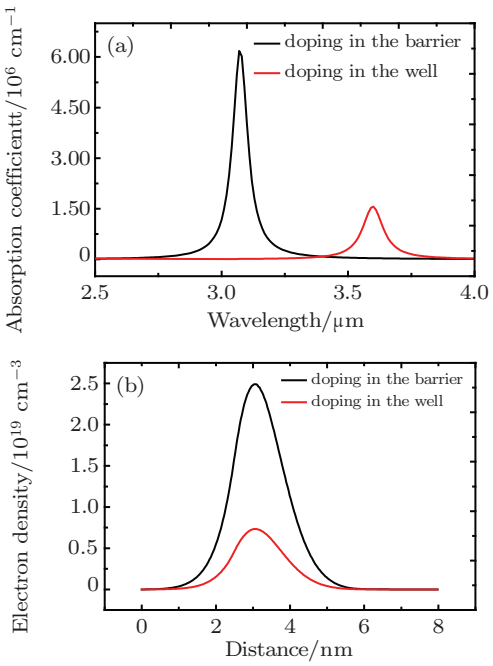


Fig. 8. (color online) (a) Absorption coefficients of structures with doping in the barrier or in the well; (b) electron densities of those structures.

Because doping Si in the AlGaN material transforms compression stress into tensile stress, which could degenerate the crystal quality,[31,32] taking both crystal quality and ease of fabrication into consideration, it is better to dope the well. This part will discuss the effects of the doping density in the well on the transitions. As shown in Fig. 9, with increasing dopant concentration, the wavelength blue shifts, which can be attributed to many body effects. It has been reported that a large number of electrons in the well could screen the polarization field in the well,[33] which could decrease the transition energy. However, because of many body effects, particularly the exchange–correlation energy and the depolarization shift, the positions of e_1 and e_2 are changed significantly. The exchange–correlation effect leads to a decrease of e_1 without e_2 changing much,[24,34] and the depolarization shift also contributes to the increase of the energy space between e_1 and e_2.[35] Thus, the transition wavelength is blue shifted when the doping density is increased. So changing the doping concentration influences the transitions significantly, which can be used as a method to tune the wavelength in the MQWs.

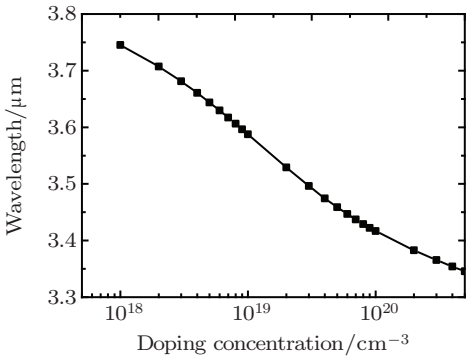


Fig. 9. Intersubband transition wavelength of the structure with different doping concentration in the well.

4. Conclusion

The effects of polarization on the intersubband transitions of $Al_{0.35}Ga_{0.65}N$/GaN MQWs have been investigated. The results show that the absorption coefficient increases with increasing polarization while the transition wavelength decreases, which is not identical to the cases of interband transitions. This difference can be attributed to the fact that the triangular well caused by the electrostatic field enhances the confinement of electrons and enlarges the energy space between e_1 and e_2. Moreover, the influences of parameters such as barrier thickness, well width, Al mole composition of barrier, and doping on the intersubband transitions in AlGaN/GaN MQWs are also investigated. The results show that the wavelength is red shifted with the increase of barrier thickness or well width while the wavelength is blue shifted when the Al mole composition is increased. Furthermore, the effects of the well width on the intersubband transitions are more dramatic than those of the barrier thickness, and the effects of the Al mole composition on the electron subband levels are not the

same. In addition, the structure with doping in the barrier has a shorter wavelength than that with doping in the well, and the wavelength blue shifts with the increase of the doping density due to many body effects. Therefore, the influences of every structural parameter of AlGaN/GaN MQWs on the transitions should be considered comprehensively when designing an infrared detector based on the AlGaN/GaN MQWs, especially the Al mole composition of the barrier and the width of the well, which affect the transitions most.

References

[1] Oh J H, Oh J R, Park H K, Sung Y G and Do Y R 2011 *Opt. Express* **19** A270

[2] Wang Z G, Chen W J, Zhang J, Zhang B and Li Z J 2012 *Chin. Phys. B* **21** 087305

[3] Liao C T, Tsai M C, Liou B T, Yen S H and KuoY K 2010 *J. Appl. Phys.* **108** 063107

[4] Zhu J, Ban S L and Ha S H 2012 *Suprelattice Microst.* **51** 471

[5] Hofstetter D, Baumann E, Giorgetta F R, Theron R, Wu H, Schaff W J, Dawlaty J, George P A, Eastman F L, Rana F, Kandaswamy P K, Guillot F and Monroy E 2010 *Proc. IEEE* **98** 1234

[6] Huang C C, Xu F J, Yan X D, Song J, Xu Z Y, Cen L B, Wang Y, Pan J H, Wang X Q, Yang Z J, Shen B, Zhang B S, Chen X S and Lu W 2011 *Appl. Phys. Lett.* **98** 132105

[7] Lei S Y, Shen B and Zhang G Y 2006 *Chin. Phys. Lett.* **23** 1574

[8] Driscoll K, Liao Y, Bhattacharyya A, Moustakas T D, Paiella R, Zhou L and Smith D J 2010 *Phys. Status Solidi C* **7** 2394

[9] Machhadani H, Kandaswamy P, Sakr S, Vardi A, Wirtmüller A, Nevou L, Guillot F, Pozzovivo G, Tchernycheva M, Lupu A, Vivien L, Crozat P, Warde E, Bougerol C, Schacham S, Strasser G, Bahir G, Monroy E and Julien F H 2009 *New J. Phys.* **11** 125023

[10] Laperne N P, Bayram C, Nguyen-The L, McClintock R and Razeghi M 2009 *Appl. Phys. Lett.* **95** 131109

[11] Machhadani H, Kotsar Y, Sakr S, Tchernycheva M, Colombelli R, Mangeney J, Bellet-Amalric E, Sarigiannidou E, Monroy E and Julien F H 2010 *Appl. Phys. Lett.* **97** 191101

[12] Gmachl C, Ng H M and Cho A Y 2000 *Appl. Phys. Lett.* **77** 334

[13] Tchernycheva M, Nevou L, Doyennette L, Julien F H and Warde E 2006 *Phys. Rev. B* **73** 125347

[14] Ahn D and Chuang S L 1987 *IEEE J. Quantum Electron.* **23** 2196

[15] Cen L B, Shen B, Qin Z X and Zhang G Y 2009 *Chin. Phys. B* **18** 3905

[16] Cen L B, Shen B, Qin Z X and Zhang G Y 2009 *J. Appl. Phys.* **105** 053106

[17] Ridley B K, Schaff W J and Eastman L F 2003 *J. Appl. Phys.* **94** 3972

[18] Vurgaftman I and Meyer J R 2003 *J. Appl. Phys.* **94** 3675

[19] Li J M, Lü Y W, Li D B, Han X X, Zhu Q S, Liu X L and Wang Z G 2004 *J. Vac. Sci. Technol. B* **22** 2568

[20] Razeghi M and McClintock R 2009 *J. Cryst. Growth* **311** 3067

[21] Allerman A A, Crawford M H, Miller M A and Lee S R 2010 *J. Cryst. Growth* **312** 756

[22] Suzuki N, Iizuka N and Kaneko K 2003 *Jpn. J. Appl. Phys.* **42** 132

[23] Hofstetter D, Baumann E, Giorgetta F R, Theron R, Wu H, Schaff W J, Dawlaty J, George P A, Eastman F L, Rana F, Kandaswamy P K, Leconte S and Monroy E 2009 *J. Phys.: Condens. Matter* **21** 174208

[24] Kandaswamy P K, Machhadani H, Kotsar Y, Sakr S, Das A, Tchernycheva M, Rapenne L, Sarigiannidou E, Julien F J and Monroy E 2010 *Appl. Phys. Lett.* **96** 141903

[25] Bayram C, Fain B, Pere-laperne N, McClintock R and Razeghi M 2009 *Proc. SPIE* **7222** 722212

[26] Kozodoy P, Hansen M, DenBaars S P and Mishra U K 1999 *Appl. Phys. Lett.* **74** 3681

[27] Kandaswamy P K, Guillot F, Bellet-Amalric E, Monroy E, Nevou L, Tchernycheva M, Michon A, Julien F H, Baumann E, Giorgetta F R, Hofstetter D, Remmele T, Albrecht M, Birner S and Dang L S 2008 *J. Appl. Phys.* **104** 093501

[28] Driscoll K, Liao Y, Bhattacharyya A, Moustakas T D, Paiella R, Zhou L and Smith D J 2010 *Phys. Status Solidi C* **7** 2394

[29] Dussaigne A, Nicolay S, Martin D, Castiglia A, Grandjean N, Nevou L, Machhadani H, Tchernycheva M, Vivien L, Julien F H, Remmele T and Albrecht M 2010 *Proc. SPIE* **7608** 76080H

[30] Yang J S, Sodabanlu H, Sugiyama M, Nakano Y and Shimogaki Y 2011 *J. Cryst. Growth* **314** 252

[31] Acord J D, Manning I C, Weng X J, Snyder D W and Redwing J M 2008 *Appl. Phys. Lett.* **93** 111910

[32] Cantu P, Wu F, Waltereit P, Keller S, Romanov A E, Mishra U K, DenBaars S P and Speck J S 2003 *Appl. Phys. Lett.* **83** 674

[33] Zhang W, Zhang Y, Xue J S, Zhang Y, Lv L, Zhang J C and Hao Y 2011 *Appl. Phys. Lett.* **99** 162105

[34] Zhang Y H and Cao J C 2005 *Chin. Phys. Lett.* **22** 2696

[35] Park S H and Ahn D 1997 *Appl. Phys. Lett.* **71** 398